Translational Oncology
www.transonc.com
Volume 4 Number 3 June 2011 pp. 173–177 173

Feasibility and Safety of Silicone Rubber Contrast-Enhanced Microcomputed Tomography in Evaluating the Angioarchitecture of Prostatectomy Specimens[1]

Alex K. Yeung, Mostafa Atri, Linda Sugar[2] and Laurence Klotz[3]

Department of Medical Imaging, Toronto General Hospital, Toronto, Ontario, Canada

Abstract

This ethics committee–approved pilot study was carried out with informed consent. A protocol was developed to assess the feasibility of *in vitro* Microfil injection of prostate cancer specimens followed by analysis with microcomputed tomography (microCT) to characterize the functional vascularity of prostatic tissue and evaluate its safety with respect to the preservation of a specimen for pathologic examination. The visible prostatic arteries of two surgically resected prostates from patients with known prostate cancer (PCa) were injected with Microfil MV-122 contrast medium immediately after removal. The specimens were scanned using microCT and were qualitatively examined using three-dimensional analysis software (MicroView; GE Healthcare Biosciences). The Microfil perfusion in the two samples was sufficient to view the functional vascularity arising from a major prostatic artery, up to a resolution of 17.626 μm without any indication of adverse effects due to Microfil injection. Malignant prostatic regions showed a greater vascular density on histology but decreased vascular perfusion compared with benign prostatic regions. The use of microCT on Microfil-injected prostates seems to be a feasible and specimen-preserving method for visualizing the three-dimensional vessel patterns present in resected human prostates.

Translational Oncology (2011) 4, 173–177

Introduction

Many techniques using different cross-sectional modalities are currently being evaluated for the image-guided treatment of prostate cancer. Two of these use ultrasound and magnetic resonance imaging (MRI), combined with contrast agents [1,2]. One of the major limiting factors of these techniques is uncertainty regarding their ability to delineate the functional (patent) vascularity of prostate cancer (PCa).

This study uses a low-viscosity radiopaque polymer, Microfil MV-122 (Flow Tech, Inc, Carver, MA), which is ideal for enabling more accurate assessments of prostatic patent angioarchitecture. Microfil has the advantage of being easy to handle compared with other contrast agents such as barium sulfate in gelatin; this is because Microfil's contrast particles do not settle as quickly, permitting more time for accurate and thorough vascular perfusion. Furthermore, use of Microfil avoids the tissue degradation and vessel loss due to breakage, which is commonly associated with vessel enhancement achieved through vascular cast corrosion [3]. Microfil has previously been used to characterize the importance of vascular endothelial growth factor in angiogenesis during tumor proliferation and maintenance [4] and to reveal morphologic differences in splenic tumor angiogenesis [5]. The compound has also been combined with microcomputed tomography (microCT) to demonstrate the high visual correlation with results from a T1-weighted MRI scan in a mouse's brain tumor vasculature [6] as well as to assess the functional vasculature in a mouse model

Address all correspondence to: Dr. Mostafa Atri, Department of Medical Imaging, Toronto General Hospital, Room NCSB 1C569, 585 University Ave, Toronto, Ontario, Canada M5G 2N2. E-mail: mostafa.atri@uhn.on.ca

[1]A.K. Yeung received grant support from the Radiological Society of North America's Research Medical Student Grant and the Queen's University JD Hatcher Award.

[2]Current address: Department of Anatomic Pathology, Sunnybrook Health Sciences Centre, 2075 Bayview Ave, Toronto, Ontario, Canada M4N 3M5.
[3]Current address: Department of Surgery, Sunnybrook Health Sciences Centre, 2075 Bayview Ave, Toronto, Ontario, Canada M4N 3M5.

Received 31 December 2010; Revised 24 March 2011; Accepted 24 March 2011

1944-7124/11
DOI 10.1593/tlo.10304

of PCa [7]. The angioarchitecture of many human cancers have been investigated with Microfil including an angiodysplastic right colon [8], superficial esophageal carcinoma [9], renal clear cell carcinoma [10], and small liver metastases [11]. The studies that included histologic analyses after Microfil injection did not report any adverse effects on the pathologic specimens [10,11]. Despite the wide range of studies, there is no report regarding the feasibility and safety of using and analyzing the *in vitro* Microfil-injected human prostate.

This study will evaluate the feasibility and safety of using Microfil and microCT to visualize the patent vascularity of human prostate specimens. Such information could help increase the sensitivity and specificity of vascularity-dependent imaging techniques and improve diagnostic and therapeutic capabilities.

Materials and Methods

Radical prostatectomy specimens were acquired from two consenting males aged 62 and 63 years, who had biopsy-proven prostate cancer, after ethics approval was obtained.

Prostatectomies were conducted using standard open-surgery techniques. Surgeons were specifically asked to staple or suture any visible superficial vessels seen on the prostate to allow them to be more easily detected. Prostatic arteries were dissected within 30 to 60 minutes after prostatectomy; a dissecting microscope was sometimes useful in confirming a vessel lumen or in distinguishing between veins and arteries. Arteries could often be distinguished from veins due to their thicker, white vascular walls. Branches of the prostatic arteries on the prostate's anterolateral surface [12] were cannulated with blunt-ended 27-gauge cannulae in the direction that would permit fluids to be injected intraprostatically; typically, for vessel lumens near the prostate surface, the cannulae would be oriented in a medial-posterior direction.

Immediately after cannulation, heparinized saline (20°C, 400 IU/ml) was manually injected through the cannulae, at a pressure that offered slight resistance. This was done to avoid *ex vivo* coagulation and performed until the perfusate was free of blood; approximately 200 ml was used to achieve this. The heparinized saline was also used to rinse the specimen's external surface to remove extraneous blood.

At this point, the low-viscosity Microfil was prepared in a syringe by mixing 5 ml of Microfil MV-122 with 5 ml of diluent, as well as 1 ml of curing agent that had been heated to ~40°C. The syringe was then attached to the manual pump setup.

The pump was used to maintain a pressure of 120 to 180 mm Hg, which is similar to the pressures used by other Microfil-using researchers to effectively perfuse other organs at a similar viscosity to blood [3,4,13] and is within the 100- to 200-mm Hg range that Clegg [14] used when he characterized the prostate vasculature with an injected barium sulfate compound. The physiological-like pressure range was used to perfuse the Microfil into the prostate specimen, through branches of the prostatic arteries. Each cannulated vessel was serially attached to the syringe and had Microfil pumped through it, in an attempt to ensure optimal Microfil perfusion into the prostatic vessels. Microfil was injected until it was seen continuously exiting the prostate from other open vessels on the surface of the prostate, or until there was enough backward pressure on the cannula to begin to cause the ejection of the cannula. Periodic movement of the cannula to different vessel depths, and recannulating the same vessel, allowed the user to ensure that the tip of the cannula was not obstructed by a vessel wall and to confirm that the Microfil had not yet cured and was still flowing.

There is an approximately 20-minute window of working time before the Microfil will cure based on the composition described. Once the Microfil had cured in the syringe and was no longer flowing out of the cannula, the specimen sat for an additional 60 minutes to guarantee that the remaining contrast agent would cure. At this point, formalin was applied to rinse off the remaining surface-bound Microfil, in addition to fixing the specimen for 2 to 6 days. During this period, microCT scans of the specimen were performed in air using an Inveon CT Module (Siemens Medical Solutions, Erlangen, Germany). The scanning parameters used were as follows: kilovolt (peak) = 80 keV, x-ray tube current = 0.5 mA, exposure = 3500 to 3900 milliseconds per view, magnification = low, voxel size = 26.263 μm × 26.263 μm × 26.263 μm (one prostate was scanned at 17.626 μm × 17.626 μm × 17.626 μm), number of views = 360 degrees over 360 degrees, scan time = ~24 minutes, number of reconstructed voxels = 2048 × 2048 × 2272 (max *z*-axis value = 3072), and reconstruction time = ~6 hours.

The resultant microCT images were reconstructed three-dimensionally, and the vascular patterns were examined using MicroView (GE Healthcare Biosciences, Buckinghamshire, UK).

After the microCT scans, the prostatectomy specimens were sectioned and histologically examined by a pathologist (L.S.). This was done to stage and grade the PCa and, with the use of CD31 immunohistochemistry markers, to identify any adverse tissue effects due to the presence of the Microfil. Moreover, the CD31 staining allowed the quantification of vessel densities at 40× magnification in both benign and malignant tissues; vessels were registered regardless of whether they were associated with a visible lumen. Gross pathology and histologic pictures were acquired and reviewed at 10× magnification to demonstrate the presence and patterns of vascular Microfil.

Results

Two radical prostatectomy specimens were successfully perfused with the Microfil.

Figure 1*A* shows the gross appearance of one of the prostate specimens that was successfully perfused on one side using the Microfil compound. Two of the anterolateral prostatic vessels were identified and cannulated on one side to achieve the perfusion. When examined using microCT, a corkscrew-like appearance was noted in some surface vessels. These vascular patterns agree with observations originally described by Clegg [14], who regarded them as being associated with benign tissues and possibly due to smooth muscle variations in those regions. Figure 1*B* shows a coronal section of the same prostate that was injected unilaterally with the Microfil. Findings from the other prostate resembled those of Figure 1*A*, particularly regarding the presence of prostatic surface vessels displaying corkscrew-like patterns.

Figure 2 shows a three-dimensional microCT maximum-intensity projection of the prostate in Figure 1, injected unilaterally with the Microfil. It is evident that there is widespread vascularization infiltrating into one side of the prostate specimen. The vascularization pattern also supports the idea of end-capillary angioarchitecture [12], as each cannulation site supplied its own set of vessels. It is believed that the smaller vessels where Microfil was seen exiting from, after injection of the Microfil into a cannulated vessel, are branches off the main cannulated vessel that had tunneled to the prostate surface and opened up (through trauma) during the prostate resection.

Histologic analysis of the specimens for grading and staging of PCa was also achieved, without any indication of adverse effects from this study's technique. Microfil-laden vessels in the vicinity of both

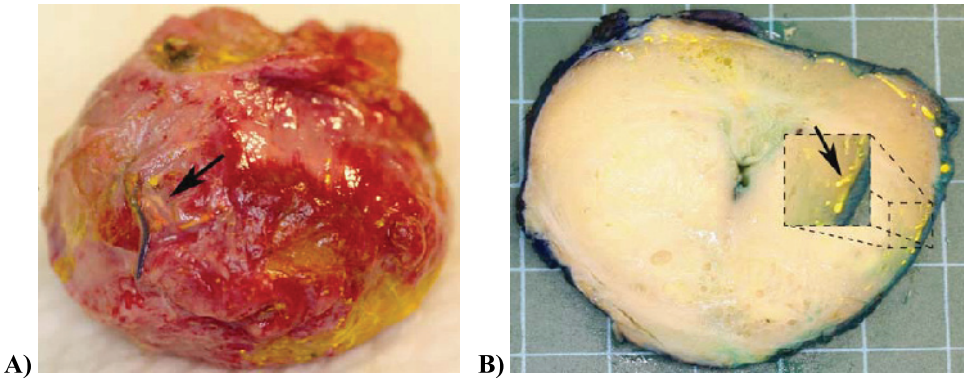

Figure 1. (A) Gross specimen of a prostate, unilaterally injected with Microfil MV-122. Arrow tip indicates superficial vessels perfused with Microfil MV-122 (yellow). (B) Gross specimen of a coronal section of a prostate, unilaterally injected with Microfil MV-122 into a branch of the prostatic artery. Arrow tip indicates capsular vessel perfused with Microfil MV-122 (yellow).

malignant and benign tissues were seen in the specimens, revealing vessel diameters as small as 18 μm. Areas of higher Microfil perfusion tended to involve nonmalignant tissue exhibiting 3 to 79 Microfil-containing vessels per 25 fields at 10× power, whereas areas of reduced Microfil perfusion were often seen in malignant tissues ranging from as few as 1 Microfil-containing vessel per 14 fields to as high as 8 Microfil-containing vessels per 25 fields at 10× power (P = .066) (Table 1). The number of fields examined for malignant tissue was different from benign tissue because of the paucity of Microfil-containing malignant vessels. Although the dissimilarities in Microfil-containing vessel densities did not reach significant statistical difference, it suggests a trend, and the lack of significant difference could be related to the small sample size. Furthermore, at 40× magnification, increased vascular density was apparent in malignant *versus* benign CD31-stained prostatectomy tissues. On average, there were approximately 60 vessels in malignant tissues compared to approximately 33 vessels in benign tissues, per 40× high-power field (P < .0001) (Table 2). It was also observed that many vessels in the malignant areas, as demonstrated by CD31 immunostaining, were very tiny and did not possess readily identifiable lumens.

Figure 3 demonstrates the appearance of Microfil within intraprostatic vessels. The Microfil appears black due to the hematoxylin-eosin staining. It also appears shrunken in the vessels, which is attributed to the pathologic processing of the specimen. The fact that the blood found in the lumen of vessels, which had not been cleared with the heparin-saline solution, was shrunken away from the vessel walls supports this, in addition to the observations of shrunken Microfil in the histologic images acquired from other researchers [5,8,11]. No visible signs of Microfil leakage into the interstitial space or lymphovascular channels were observed histologically—if this had occurred in the former, it is expected that the Microfil would be readily seen in pooled non–tubular-shaped conformations.

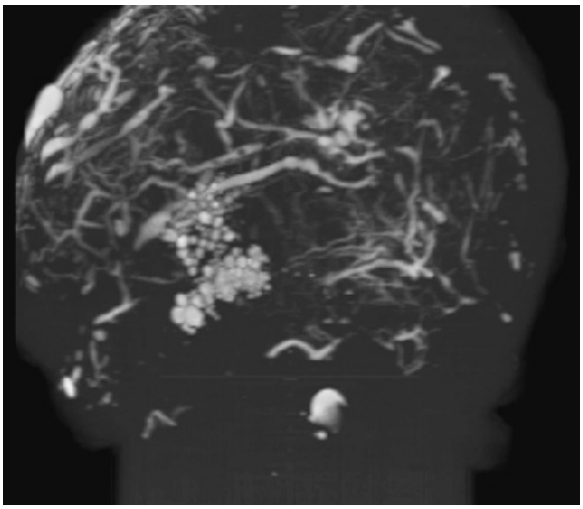

Figure 2. Three-dimensional microCT maximum-intensity projection of a prostate unilaterally injected with Microfil into a branch of the prostatic artery. The central nodular densities are believed to be artifacts, as they were located in a benign area of the prostate specimen and no pathology equivalent was observed.

Discussion

Several studies have attempted to characterize the prostatic vasculature. However, few offer techniques that are both effective and safe. Slojewski et al. [15] injected a prostate specimen containing PCa using a technically difficult and time-consuming procedure involving finely ground barium sulfate, which required three times as many unsuccessful attempts for every successfully injected prostate. Neumaier et al. [12], who used color Doppler ultrasound to examine prostate vasculature *in vivo*, found that their technique was problematic due to interference caused by tissues and vessels surrounding, and preceding, the prostatic vessels. The use of Microfil and microCT in the current study avoids such problems because Microfil is nontoxic and microCT readily distinguishes between opaque Microfil-injected vessels and their surrounding less-dense tissues.

Table 1. Quantification of Microfil-Containing Vessels at 10× Magnification, from Two Microfil-Injected Prostatectomy Specimens.

	[Number of Microfil-Containing Vessels] / [Number of Fields] at 10× Power		
	Specimen 1	Specimen 2	Mean ± SD
Malignant tissues	1/14, 1/14, 1/14	8/25, 8/25, 5/22	[4.51 ± 3.1] / 25
Benign tissues	13/25, 4/25, 9/25, 3/25, 79/25, 10/25	12/25, 12/25, 16/25, 57/25	[21.5 ± 25.4] / 25

Random samples from both malignant and benign tissues were assessed for each prostatectomy specimen, with a variable number of fields counted per slide. t_9 = 2.09, P = .066.

Table 2. Quantification of CD31-Stained Vessels at 40× Magnification, from Two Microfil-Injected Prostatectomy Specimens.

	Number of Vessels per 40× HPF		
	Specimen 1	Specimen 2	Mean ± SD
Malignant tissues	70, 65, 53	53, 57, 60	59.7 ± 6.8
Benign tissues	22, 32, 35	38, 30, 38	32.5 ± 6.1

Three random samples from both malignant and benign tissues were assessed for each prostatectomy specimen. $t_{10} = -7.31$, $P < .0001$. HPF indicates high-power field.

In this study, the vessels observed on microCT could be as small as 17.626 μm in diameter. This is much more sensitive than other techniques such as power Doppler, which has a detection limit of ~100 to 150 μm [7]. It has been found that, in androgen-dependent Shionogi carcinomas, which may resemble the androgen-sensitive PCa tissues, vessels ranged in size from 4.3 to 143 μm with average diameters of 20 μm [16]. Consequently, this study's technique could provide an accurate display of the patent angioarchitecture in PCa tissues. It is important to note that large amounts of computer storage and power are also necessary to process the higher-resolution images achievable with this protocol. In our case, one specimen scanned with 17.626 μm voxel resolution required more than 20 GB of storage space and could only be viewed in sections as the entire specimen required a minimum of 20.032 GB of RAM to be viewed in MicroView.

There were no visible adverse effects on the specimens due to the Microfil, and no signs of Microfil leakage into the interstitial space or lymphovascular channels were observed histologically. Potential problems with identifying and correctly cannulating branches of the prostatic arteries will resolve once more specimens are assessed, and familiarity is acquired, with this technique.

Comparisons of the microvascular densities of benign and malignant foci using CD31 staining showed higher microvascular density in the malignant tissues, which reached statistical significance ($P < .0001$). However, there was reduced Microfil-laden vessels in the malignant tissues compared with benign, and although this did not reach statistical significance ($P = .06$), likely because of the small sample size, it suggests a trend. This may be due to abnormal heterogeneous vasculature (i.e., vessel angulations) and microenvironments (i.e., elevated interstitial fluid pressures) expected in malignant tissues [17]. Nonpatent malignant vascular lumens are another possibility because only 20% of tumor vessels may be actually patent [18]. This is supported by this study's findings, which revealed that many CD31-immunostained vessels in malignant regions were very tiny and did not have an apparent lumen. Such traits are alleged to perpetuate angiogenesis through heterogeneous perfusion and hypoxia and are often pathognomonic for malignant vascular networks [9–11]. This observed tissue-dependent nature of prostatic patent angioarchitecture is expected to be further defined as more data are gathered with the use of the Microfil technique. The potential presence of functionally nonpatent vessels in PCa despite increased microvessel density has implications in the use of contrast-enhanced imaging to evaluate prostate cancer vascularity, especially if an intravascular contrast agent is used, such as in dynamic contrast-enhanced MRI.

In summary, our protocol provides a safe technique for the high-resolution examination of the functional vasculature of prostate specimens. This protocol preserves the surrounding tissues so that the specimens may still undergo pathologic processing necessary for grading and staging of the cancer after their vascular assessment. The fact that this study's protocol focuses on the functional vasculature could enable more definitive conclusions to be drawn with regard to the vascularity of a tumor seen on imaging, compared with the mean vascular density that identifies both patent and nonpatent vessels. Quantitative analyses of such patterns can be easily achieved using microCT images, which are able to capture a precise cast of the angioarchitecture of prostate specimens. Analysis of larger numbers of specimens using this protocol could provide more definitive data to recognize, and potentially predict, malignant from benign prostatic tissues to aid imaging distinction.

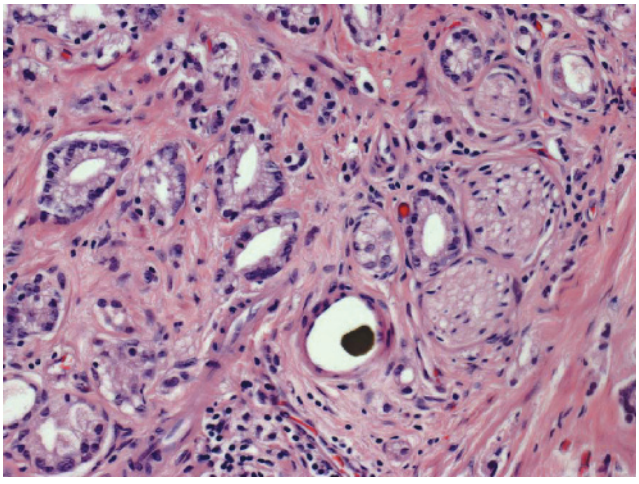

Figure 3. Histologic appearance of dark-colored Microfil in an intraprostatic vessel, situated in malignant tissues.

Acknowledgments

The authors gratefully acknowledge the help of Xiuling Qi (Sunnybrook Health Sciences Centre) and Jinzi Zheng, MASc (MaRS Centre), for their contributions in experimental technique and microCT specimen scanning, respectively.

References

[1] Simpson DH, Burns PN, and Averkiou MA (2001). Techniques for perfusion imaging with microbubble contrast agents. *IEEE Trans Ultrason Ferroelectr Freq Control* **48**, 1483–1494.

[2] Choi YJ, Kim JK, Kim N, Kim KW, Choi EK, and Cho KS (2007). Functional MR imaging of prostate cancer. *Radiographics* **27**(1), 63–75.

[3] Marxen M, Thornton MM, Chiarot CB, Klement G, Koprivnikar J, Sled JG, and Henkelman RM (2004). MicroCT scanner performance and considerations for vascular specimen imaging. *Med Phys* **31**(2), 305–313.

[4] Grunstein J, Masbad JJ, Hickey R, Giordano F, and Johnson RS (2000). Isoforms of vascular endothelial growth factor act in a coordinate fashion to recruit and expand tumor vasculature. *Mol Cell Biol* **20**(19), 7282–7291.

[5] Sasaki K, Kiuchi Y, Sato Y, and Yamamori S (1991). Morphological analysis of neovascularization at early stages of rat splenic autografts in comparison with tumor angiogenesis. *Cell Tissue Res* **265**(3), 503–510.

[6] Bock NA, Zadeh G, Davidson LM, Qian B, Sled JG, Guha A, and Henkelman RM (2003). High-resolution longitudinal screening with magnetic resonance imaging in a murine brain cancer model. *Neoplasia* **5**(6), 546–554.

[7] Xuan JW, Bygrave M, Jiang H, Valiyeva F, Dunmore-Buyze J, Holdsworth DW, Izawa JI, Bauman G, Moussa M, Winter SF, et al. (2007). Functional neoangiogenesis imaging of genetically engineered mouse prostate cancer using three-dimensional power Doppler ultrasound. *Cancer Res* **67**(6), 2830–2839.

[8] Baum S, Athanasoulis CA, Waltman AC, Galdabini J, Schapiro RH, Warshaw AL, and Ottinger LW (1977). Angiodysplasia of the right colon: a cause of gastrointestinal bleeding. *AJR Am J Roentgenol* **129**(5), 789–794.

[9] Kumagai Y, Inoue H, Nagai K, Kawano T, and Iwai T (2002). Magnifying endoscopy, stereoscopic microscopy, and the microvascular architecture of superficial esophageal carcinoma. *Endoscopy* **34**(5), 369–375.

[10] Bugajski A, Nowogrodzka-Zagorska M, Lenko J, and Miodonski AJ (1989). Angiomorphology of the human renal clear cell carcinoma. A light and scanning electron microscopic study. *Virchows Arch A Pathol Anat Histopathol* **415**(2), 103–113.

[11] Lin G, Boijsen E, Hagerstrand I, and Lunderquist A (1984). Microvasculature architecture of small liver metastases in man. A correlation between microfil vascular preparations and histologic sections. *Invest Radiol* **19**(4), 296–302.

[12] Neumaier CE, Martinoli C, Derchi LE, Silvestri E, and Rosenberg I (1995). Normal prostate gland: examination with color Doppler US. *Radiology* **196**(2), 453–457.

[13] Shoshany G, Har-Shai Y, Ramon I, Bar-Maor JA, and Kimura K (1994). The isolated bowel segment: angiographic visualization of the developing vascularity. *Pediatr Surg Int* **9**(4), 261–263.

[14] Clegg EJ (1955). The arterial supply of the human prostate and seminal vesicles. *J Anat* **89**, 209–217.

[15] Slojewski M, Czerwinski F, and Sikorski A (2002). Microangiographic imaging of the prostate. *BJU Int* **89**(7), 776–778.

[16] Jain RK, Safabakhsh N, Sckell A, Chen Y, Jiang P, Benjamin L, Yuan F, and Keshet E (1998). Endothelial cell death, angiogenesis, and microvascular function after castration in an androgen-dependent tumor: role of vascular endothelial growth factor. *Proc Natl Acad Sci USA* **95**(18), 10820–10825.

[17] Lunt SJ, Chaudary N, and Hill RP (2009). The tumor microenvironment and metastatic disease. *Clin Exp Metastasis* **26**(1), 19–34.

[18] Delorme S and Knopp MV (1998). Non-invasive vascular imaging: assessing tumour vascularity. *Eur Radiol* **8**(4), 517–527.